

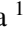



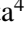




Investigation of Deep Neural Network Compression Based on Tucker Decomposition for the Classification of Lesions in Cavity Oral

Vitor B. L. Fernandes¹^a, Adriano B. Silva¹^b, Danilo C. Pereira¹^c, Sérgio V. Cardoso²^d, Paulo R. de Faria³^e, Adriano M. Loyola²^f, Thaína A. A. Tosta⁴^g, Leandro A. Neves⁵^h and Marcelo Z. do Nascimento¹ⁱ

¹Faculty of Computer Science, Federal University of Uberlândia, Brazil

²Area of Oral Pathology, School of Dentistry, Federal University of Uberlândia, Brazil

³Department of Histology and Morphology, Institute of Biomedical Science, Federal University of Uberlândia, Brazil

⁴Science and Technology Institute, Federal University of São Paulo, Brazil

⁵Department of Computer Science and Statistics (DCCE), São Paulo State University, Brazil


Keywords: Oral Epithelial Dysplasia, Convolutional Neural Network, Tensors, Histological Image, Classifier, Tucker Decomposition.


Abstract: Cancer in the oral cavity is one of the most common, making it necessary to investigate lesions that could develop into cancer. Initial stage lesions, called dysplasia, can develop into more severe stages of the disease and are characterized by variations in the shape and size of the nucleus of epithelial tissue cells. Due to advances in the areas of digital image processing and artificial intelligence, diagnostic aid systems (CAD) have become a tool to help reduce the difficulties of analyzing and classifying lesions. This paper presents an investigation of the Tucker decomposition in tensors for different CNN models to classify dysplasia in histological images of the oral cavity. In addition to the Tucker decomposition, this study investigates the normalization of H&E dyes on the optimized CNN models to evaluate the behavior of the architectures in the classification stage of dysplasia lesions. The results show that for some of the optimized models, the use of normalization contributed to the performance of the CNNs for classifying dysplasia lesions. However, when the features obtained from the final layers of the CNNs associated with the machine learning algorithms were analyzed, it was noted that the normalization process affected performance during classification.


1 INTRODUCTION


Oral cavity cancer is one type common accounting for almost 50% of cases in the head and neck region (Wild et al., 2020). This highlights the importance of investigating lesions that may develop into cancer. One of such lesions, known as dysplasia, is characterized by changes in the shape and size of the nuclei of epithelial cells (Kumar et al., 2009).


With advances in digital image processing and artificial intelligence, computer-aided diagnosis (CAD) systems have become increasingly popular and have reduced the challenges faced by healthcare professionals during tissue classification (Belsare, 2012). CAD systems encompass the stages of image enhancement, segmentation, feature extraction, and classification. In (Ferro et al., 2022), the authors present the machine learning methods addressed for the implementation of automated detection of potentially malignant and malignant diseases of the oral cavity. In recent years, these systems adopted deep learning-based strategies, such as convolutional neural networks, to improve these stages. Despite their relevant contributions, these systems are often impacted by over-parameterization. This high number of parameters can be optimized using tensor decomposition techniques applied to the convolutional layers


^a <https://orcid.org/0009-0007-8230-8779>


^b <https://orcid.org/0000-0001-8999-1135>


^c <https://orcid.org/0000-0002-2694-4865>


^d <https://orcid.org/0000-0003-1809-0617>

^e <https://orcid.org/0000-0003-2650-3960>

^f <https://orcid.org/0000-0001-9707-9365>

^g <https://orcid.org/0000-0002-9291-8892>

^h <https://orcid.org/0000-0001-8580-7054>

ⁱ <https://orcid.org/0000-0003-3537-0178>

kernels, aiming to reduce the total number of parameters in the network (Kim et al., 2016). The authors in (Liu and Ng, 2022) pointed out that further research is needed to investigate convolutional neural network (CNN) model compression, in order to reduce parameter amount while maintaining the same accuracy as the original model.

Another factor that can reduce the performance of classification methods used in CAD systems is related to the pre-processing stage (Ribeiro et al., 2018). During the process of obtaining digital histological images, slides are stained with hematoxylin–eosin (H&E), in which the hematoxylin dye stains acid structures in purple and the eosin dye stains the basic ones in pink (Celis and Romero, 2015a). This process can present non-uniformity in the distribution of dyes along the tissue. The use of different fixatives, digitization equipment, and differences in the slide storage are examples of factors that lead to color variations on these images (Tosta et al., 2019a). Therefore, exploring the impact of H&E dye normalization on histological dysplasia tissues in the context of dysplasia classification of optimized CNN models remains an ongoing challenge.

This paper presents an investigation of Tucker decomposition in tensors of ResNet-18 and ResNet-50 CNN architectures for the classification of dysplasias in histological images of the oral cavity. Moreover, this study investigates the normalization of H&E dyes on optimized models to evaluate their behavior in the classification stage. At last, the feature extraction stage was performed in non-normalized and color-normalized images obtained from the previous convolutional layer to assess the color-normalization impact on the classification stage using machine learning algorithms. Thus, the main contributions are:

- Study of the Tucker decomposition technique for use with ResNet architecture tensors for evaluation in the classification of dysplasia lesions;
- Investigation of the impact of color normalization in dysplasia classification using ResNet model;
- Analysis of the features from the global average pooling layer, before the fully connected layer of the ResNet models for, classifying dysplasia lesions using machine learning (ML) algorithms.

2 METHODOLOGY

Figure 1 shows the sequence of steps performed to classify dysplasia lesions on the models investigated. All the experiments carried out in this work were conducted on a machine with an AMD Ryzen 5 3600XT

processor, GeForce RTX 2070 SUPER graphics card, and 64GB of RAM.

2.1 Image Dataset

The dataset consists of 30 H&E-stained mice tongue tissue sections previously submitted to a carcinogen during two experiments carried out in 2009 and 2010. These experiments were approved by the Ethics Committee on the Use of Animals under protocol number 038/09 at the Federal University of Uberlândia, Brazil.

The histological slides were digitized using the Leica DM500 optical microscope with 400× magnification. A total of 66 images were obtained and stored in the TIFF format using the RGB color model with a resolution of 2048×1536 pixels. Using the methodology described by (Lumerman et al., 1995), the images were classified between healthy and severe OED images. From the images, 74 ROIs of size 450 × 250 pixels were obtained for each class. Examples of these ROIs can be seen in Figure 2.

2.2 H&E Stain Normalization

Color normalization is a process applied at the stage of image processing aiming to reduce possible color variations between samples that may arise during the digitization and staining stages (Sha et al., 2017). In literature, several techniques are described for color normalization, such as those proposed by (Vahadane et al., 2015) and (Tosta et al., 2019b).

In this work, the technique proposed by (Tosta et al., 2019b) was employed. This technique was developed specifically to normalize H&E dyed histological images. Hematoxylin stains the nuclei with purple color and eosin colors the cytoplasm and other extracellular structures as pink (Celis and Romero, 2015b). However, the color obtained in the images can undergo variations depending on other factors, such as the way the image was digitized and how the preparation was performed (Khan et al., 2014; Sethi et al., 2016).

The adopted approach normalizes the image colors while maintaining the histological structures and ensuring that no artifacts are introduced (Tosta et al., 2019b). The method achieves this result with an unsupervised estimate of the sparsity parameter and stain representation.

2.3 ResNet Architecture

The CNN architectures used in the experiments were ResNet models. This architecture was proposed

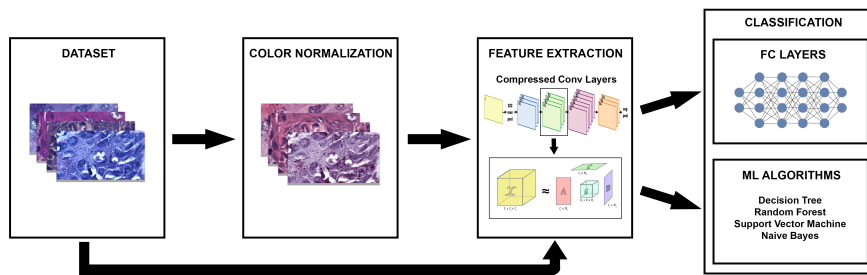


Figure 1: Box diagram of the stages employed for the classification of oral dysplasia tissue images.

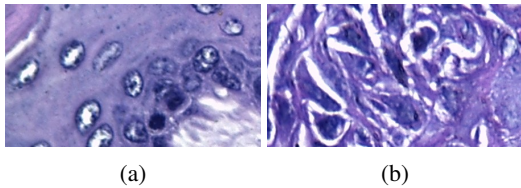


Figure 2: Examples of oral histological tissues: (a) healthy tissue; (b) severe dysplasia.

in (He et al., 2015) and it is a deep convolutional neural network model based on the use of the so-called residual learning. Residual learning consists of skipping one or more layers, keeping the information intact, and then applying it to the output of subsequent layers. This approach helps to improve the performance of the network over many layers by avoiding the degradation problem that can occur with other architectures.

The ResNet architecture is available in different versions, with different numbers of layers. For this study's experiments, ResNet-18 and ResNet-50 models were chosen, which have 18 and 50 layers, respectively. The choice of this architecture was motivated by two reasons. The first is that it has been widely used in other studies of histological images, such as the classification of images from different body parts (Talo, 2019), the performance of both ResNet-18 and ResNet-50 in the classification of colorectal cancer images (Sarwinda et al., 2021) and research that proposed the use of ResNet-50 for classification breast cancer images (Al-Haija and Adebajo, 2020). The second reason was due to its structure, which is mostly composed of convolutional layers. As decomposition techniques are applied only to convolutional layer tensors, using a network that has relatively few parameters in densely connected layers ensures that the decomposition is more expressive.

2.4 Tucker Decomposition

Tensor is a concept used primarily in computing as a generalization of a matrix to dimensions greater than three. A tensor with one dimension is typically called

a vector. A tensor with two dimensions is called a matrix. From three dimensions, the used term simply becomes tensor and can refer to an N -th-order tensor, with N being the number of dimensions present in that tensor (Kolda and Bader, 2009). Tensors play an important role in several areas of computing, being mainly used in signal processing techniques, ML, clustering and dimensionality reduction algorithms, and data mining (Sidiropoulos et al., 2017).

A tensor of many dimensions can undergo a series of mathematical transformations to rearrange its format and result in more than one tensor while maintaining an approximation of the information contained in the original tensor. This operation is called low-rank approximation (Kolda and Bader, 2009). After applying this operation, the resulting tensors have fewer parameters than the original one, resulting in a reduction in dimensionality and the total number of parameters. An approximation of the original tensor can be obtained from operations applied to the resulting tensors (Cichocki et al., 2017). The quality of these approximations is dependent on the rank values chosen at the decomposition time and, depending on the situation, lower than ideal values can be used to achieve greater compression, in which the approximation does not need to be too precise (Kim et al., 2016).

There are several techniques for tensor decomposition, with the most popular being CP-Decomposition and Tucker Decomposition (Kolda and Bader, 2009). The method chosen for this study was Tucker Decomposition, which decomposes an n -dimensional tensor into $n+1$ matrices, one of which is a nucleus. The dimensions size of these matrices is based on the size of the dimensions from the original tensor and the value defined as decomposition *rank* (Kim et al., 2016).

Equation 1 defines the Tucker decomposition for a three-dimensional tensor \mathcal{X} , whose dimensions have values I_1 , I_2 and I_3 , therefore $\mathcal{X} \in R^{I_1 \times I_2 \times I_3}$, and the chosen rank values were R_1 , R_2 and R_3 :

$$\mathcal{X} \approx \mathcal{G} \times_1 A \times_2 B \times_3 C \quad (1)$$

After the decomposition, three matrices were obtained, $A \in \mathbb{R}^{I_1 \times R_1}$, $B \in \mathbb{R}^{I_2 \times R_2}$, $C \in \mathbb{R}^{I_3 \times R_3}$, and a three-dimensional nucleus $G \in \mathbb{R}^{R_1 \times R_2 \times R_3}$.

In our application, the reconstruction is not applied, since the goal is to maintain the approximation using a smaller number of parameters than the original tensor, and the reconstruction would restore the original dimensions. Even without reconstruction, performing convolutions consecutively on the new tensors resulted in weights similar to that of the original tensor. The rank values used in the experiments were defined empirically, being proportional to 0.50, 0.40, 0.30, 0.20, and 0.10 of the original values of the tensor to be decomposed. These intervals allow the evaluation of different network compression levels and the consequences of using smaller and larger rank values.

2.5 Machine Learning Algorithms

In these experiments, the data was extracted from the global average pooling layer before the fully connected layer and stored in feature vectors. Then, the ML algorithms were used to evaluate the classification of feature vectors (Wright et al., 2016). At this stage, the algorithms were implemented using the scikit-learn machine learning library.

The decision tree (DT) algorithm is a machine learning method that utilizes classification rules and analyzes data through a tree-like data structure. This structure is often represented as a tree diagram, as originally introduced by Quinlan (Quinlan, 1986). The random forest (RF) is an approach that constructs extensive collections of random decision trees to make predictions, as originally proposed by Breiman (Breiman, 2001). This method involves creating regression trees using bootstrapped samples from a training dataset, with the additional twist of selecting random features during the tree creation process. The support vector machine (SVM) algorithm is a machine learning model commonly employed in binary classification tasks. It operates by mapping input features into a multidimensional space, where it constructs a decision surface. Cortes and Vapnik (Cortes and Vapnik, 1995) presented an implementation in which it was possible to classify non-linear classes using a larger dimensional space for data classification. Thus, the tests were performed with the SVM using the polynomial kernel. The Naive Bayes (NB) method is a machine learning classification method known for its simplicity and effectiveness. It leverages Bayes' theorem, which calculates the probability of an event by considering prior knowledge of relevant conditions (Mitchell, 1997). In the classification

context, NB predicts the likelihood that a data point belongs to a specific class based on its available features and attributes

2.6 Experimental Evaluation

For the execution of the experiments, the image dataset was classified in a binary way, using only images of healthy tissues and images of severe dysplasia. The dataset was evaluated with and without normalization techniques, to verify its impact on the network accuracy after the decomposition and fine-tuning processes. Furthermore, for the classification process, the k-fold cross-validation was applied with $k = 10$.

Both the networks were trained for 500 epochs for the two datasets (normalized and non-normalized). The stochastic gradient descent (SGD) method was used as an optimizer and the loss function employed was the cross-entropy. The learning rate used in the training stage was 0.001 for both models and datasets.

In this work data augmentation techniques were used to contribute to the generalization process of the networks. In the non-normalized image sets, the following were applied: i) random horizontal flip; ii) random vertical flip; iii) rotation (max. 40°); iv) random resized crop (0.80 to 0.90); v) auto contrast; vi) sharpness; vii) colorjitter; viii) brightness; ix) contrast and saturation (0.70 to 1.30). In the normalized dataset, the same operations and settings were applied, except *ColorJitter*, which was not applied to evaluate the colorization process on the images.

After training the original networks, the Tucker decomposition was employed. The decomposition operations were applied only to the convolutional layers. Since each layer has different tensor sizes, the choice of the rank value was made proportionally, defining a value between 0 and 1, which was multiplied by the original size values of each tensor dimension. If the result is not an integer, it is rounded up. To carry out the experiments, the following rank values were defined: 0.50, 0.40, 0.30, 0.20, and 0.10 to the original values for each dimension in each tensor. These values were used in the ResNet-18 and ResNet-50 models.

In addition to evaluating the performance of image classification using the fully connected layers investigated models, the image dataset was also classified using ML algorithms, to evaluate the color normalization and compression of convolutional layer. The models chosen for both (ResNet-18 and ResNet-50) were the models with a rank ratio of 0.10 of the value of the original tensor.

After choosing the models, the histological images were inputted into the convolutional layers of

both models, and the features were extracted without passing them through the fully connected layers and the Softmax function. After being extracted, these features were used to train and test the four chosen ML algorithms: DT, RF, SVM, and NB.

For the analysis of the results for classification, the value of accuracy was applied to indicate the global performance of the model (from all classifications, how much the models got right) (Martinez et al., 2003).

In the process of evaluating the optimized models, in addition to the accuracy metric, the network weights, the total number of parameters, the number of parameters in the convolutional layers, and the time spent on decomposing and fine-tuning the network were also evaluated.

3 RESULTS

3.1 Evaluation of the Classification with the CNN Models

Tables 1 and 2 present the results obtained with the dysplasia non-normalized dataset and normalized dataset. In Table 1, the ResNet-18 model had around 11 million parameters for the original backbone. After the decomposition step, using a rank ratio of 0.50, the number of parameters decreased to approximately 4 million, resulting in a reduction of around 2.66. With the rank value 0.40 of the original, the number of parameters was approximately 3 million, equivalent to a reduction of 3.75 times. In the decomposition using a rank of 0.30, the resulting network had under 2 million parameters, with a compression rate of 5.72. Using a rank of 0.20, the reduction brings the number of parameters down to 1.5 million, which is equivalent to a network 9.70 times smaller than the original network. With a rank of 0.10, the resulting model provided a number of only 500,000 parameters, which is 19 times smaller than the size of the original network. The decomposition made with a rank value of 0.50 maintained the accuracy of 100% in the image set. The original model's rank of 0.40 resulted in an accuracy of 85.71%. With rank values of 0.30 and 0.20, the accuracy was 92.85%. Finally, the Turkey decomposition using a rank value of 0.10 returned an accuracy of 100%.

For the ResNet-50 model (see Table 1), the initial number of parameters was approximately 23.5 million. After being decomposed with a rank ratio value of 0.50, the model resulted in an increase in the number of parameters to 28.5 million. Using rank 0.40, the number of parameters obtained was around 22.6

million, which means that there was a compression of parameters. This behavior was also observed at the other rank levels. The original network achieved an accuracy of 100% on the set of images without normalization. This value was maintained for the rank proportions 0.50, 0.40, 0.30 and 0.10. Only for the model with rank of 0.20 was this value reduced to 85.71%.

Using the dataset of normalized images (see Table 2), the decomposition of the CNN models used the same values for the proportion of ranks, as defined in the Experimental evaluation section, regardless of which set of images, the number of optimization parameters in each model was similar. In the case of accuracy, the original ResNet-18 model resulted in 100% for the set of normalized images. A relevant point is that the normalized images allowed the models with compression to improve their performance for other rank values in relation to the original images, resulting in an accuracy of 100%. However, only for ResNet-50 with a rank of 0.40 did this value degrade in relation to the network's performance with the original images (92.85%).

3.2 Investigation of CNN Features with ML Algorithms

The compressed ResNet-50 and ResNet-18 models with a rank of 0.10 provided relevant results with the sets of images investigated with the smallest number of parameters and the shortest processing time. Thus, the features obtained from these models were evaluated with ML algorithms.

Figures 3 (a) and 3 (b) show the accuracy values with the ML algorithms using the original CNN and compressed backbone, respectively. Figure 3 (a) shows that the classification obtained with the DT algorithm with original ResNet-18 features was not able to achieve 100% accuracy on the non-normalized dataset. For the other algorithms investigated on this model, however, when the images were normalized, this algorithm achieved an accuracy of 100%. For the other algorithms, performance was similar between the normalized data and the original data. Figure 3 (b) shows that some of the approaches reduce the results when using the features obtained from the compressed model (DT and SVM).

Accuracy values with the ML algorithms using the original ResNet-50 and compressed ResNet-50 are presented in Figures 4 (a) and Figures 4 (b), respectively. In the same way, some of the algorithms performed similarly using the original CNN model (see Figure 4 (a)). However, only the NB algorithm improved performance after the normalization process.

Table 1: Metrics achieved with convolutional neural network models for a dataset of non-normalized histological images.

Original Image Dataset					
Rank	Accuracy (%)	Parameters	Compression Rate	Time to Decompose (seconds)	Time to Fine-tune (seconds)
ResNet-18					
Original	100	11,177,538	1	-	-
0.50	100	4,205,890	2.66	7.24	57.11
0.40	85.71	2,978,663	3.75	7.01	46.01
0.30	92.85	1,953,645	5.72	6.86	43.65
0.20	92.85	1,152,867	9.70	5.98	41.91
0.10	100	566,482	19.73	3.87	40.45
ResNet-50					
Original	100	23,512,130	1	-	-
0.50	100	28,566,722	0.82	13.08	116.71
0.40	100	22,638,820	1.04	12.41	108.04
0.30	100	17,078,229	1.38	11.66	98.55
0.20	85.71	11,933,648	1.97	10.37	87.22
0.10	100	7,200,064	3.27	6.34	76.70

Table 2: Values obtained with the metrics for the convolutional neural network models with the dataset of normalized histological images.

Normalized Image Dataset					
Rank	Accuracy (%)	Parameters	Compression Rate	Time to Decompose (seconds)	Time to Fine-tune (seconds)
ResNet-18					
Original	100	11,177,538	1	-	-
0.50	100	4,205,890	2.66	7.19	57.06
0.40	100	2,978,663	3.75	7.29	49.02
0.30	100	1,953,645	5.72	7.11	46.27
0.20	100	1,152,867	9.70	6.01	44.21
0.10	100	566,482	19.73	3.50	42.87
ResNet-50					
Original	100	23,512,130	1	-	-
0.50	100	28,566,722	0.82	13.18	126.61
0.40	92.85	22,638,820	1.04	12.69	113.54
0.30	100	17,078,229	1.38	11.64	103.14
0.20	100	11,933,648	1.97	10.29	93.52
0.10	100	7,200,064	3.27	6.52	80.03

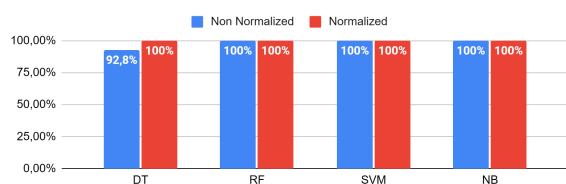
In Figures 4 (b), the features obtained from the compressed network model showed lower results when the normalization process was applied to the images for part of the classification algorithms. The results show that, although the use of stain normalization improves classification when applied only to CNN architectures, the approach of associating features and ML algorithms with data from compressed networks degraded the performance of the dataset.

Table 3 presents a comprehensive summary of the results obtained in contrast to the outcomes achieved by relevant image processing techniques developed for the examination of histopathological images of dysplasia of the oral cavity. The results show that the

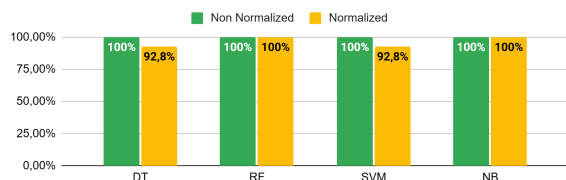
approach investigated contributes to the classification of histological lesions of the oral cavity to present a reduced CNN model to assist in the diagnostic process for specialists.

Table 3: Evaluation between proposed systems and classification methods in the literature with oral tissue dataset.

Study	Feature Extraction	Classifier	A_{CC}
(Adel et al., 2018)	ORB	SVM	92.6
(Silva et al., 2022)	CNN features	HOP	98.0
(Deif et al., 2022)	Learning feature	XGBoost	96.3
(Neves et al., 2023)	Learning feature	CNN	97.9
Proposed Approach	CNN feature	Softmax	100

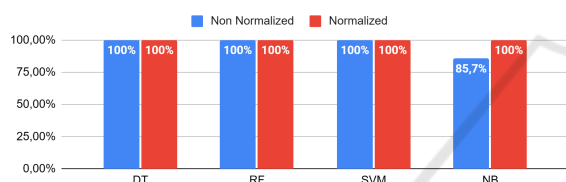


(a) Features obtained with original ResNet-18 model.

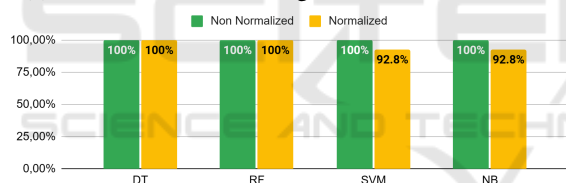


(b) Features extracted from the compressed ResNet-18 model.

Figure 3: Accuracy obtained with CNN features and ML algorithms: (a) original model; (b) compressed model.



(a) Feature obtained with original ResNet-50 backbone.



(b) Feature obtained with compressed ResNet-50 model.

Figure 4: Comparison of accuracy between the ML algorithms: (a) original model; (b) compressed model.

4 CONCLUSIONS

This work evaluated compressed ResNet architectures obtained by using Tucker decomposition on convolutional layer kernels. Furthermore, this work evaluated the impact on the accuracy of the networks when using the color normalization method proposed by (Tosta et al., 2019b) on the investigated dataset. As shown in Tables 1 and 2, the networks that were trained using our dataset achieved good accuracy, even when decomposed using very small values for the rank proportion, which resulted in significant compression of the networks, drastically reducing the total number of the parameters. These results were especially positive when combined with color normalization.

In this study, the classification also was evaluated with classic ML algorithms using the features extracted from the compressed networks. The results, shown in Figures 3 and 4, indicate that the algorithms maintain good performance in both networks when used to classify non-normalized images. However, when color normalization was applied, the algorithms demonstrated an accuracy drop, regardless of the architecture used for feature extraction. Future work will investigate other compression approaches and CNN model architectures to evaluate the classification of histological lesions

ACKNOWLEDGMENT

This study was financed in part by the Coordenação de Aperfeiçoamento de Pessoal de Nível Superior - Brasil (CAPES) - Finance Code 001. The authors gratefully acknowledge the financial support of National Council for Scientific and Technological Development CNPq (Grants #313643/2021-0, #311404/2021-9 and #307318/2022-2), the State of Minas Gerais Research Foundation - FAPEMIG (Grant #APQ-00578-18 and Grant #APQ-01129-21) and São Paulo Research Foundation - FAPESP (Grant #2022/03020-1).

REFERENCES

- Adel, D., Mounir, J., El-Shafey, M., Eldin, Y. A., El Masry, N., AbdelRaouf, A., and Abd Elhamid, I. S. (2018). Oral epithelial dysplasia computer aided diagnostic approach. In *2018 13th International Conference on Computer Engineering and Systems (ICCES)*, pages 313–318. IEEE.
- Al-Haija, Q. A. and Adebajo, A. (2020). Breast cancer diagnosis in histopathological images using resnet-50 convolutional neural network. In *2020 IEEE International IOT, Electronics and Mechatronics Conference (IEMTRONICS)*, pages 1–7.
- Belsare, A. (2012). Histopathological image analysis using image processing techniques: An overview. *Signal & Image Processing : An International Journal*, 3:23–36.
- Breiman, L. (2001). Random forests. *Machine Learning*, 45(1):5–32.
- Celis, R. and Romero, E. (2015a). Unsupervised color normalisation for h and e stained histopathology image analysis. In *11th International Symposium on Medical Information Processing and Analysis*, volume 9681, pages 16–22. SPIE.
- Celis, R. and Romero, E. (2015b). Unsupervised color normalisation for h and e stained histopathology image analysis. volume 9681. Cited by: 8.

- Cichocki, A., Phan, A.-H., Zhao, Q., Lee, N., Oseledets, I., Sugiyama, M., and Mandic, D. P. (2017). Tensor networks for dimensionality reduction and large-scale optimization: Part 2 applications and future perspectives. *Foundations and Trends® in Machine Learning*, 9(6):431–673.
- Cortes, C. and Vapnik, V. (1995). Support-vector networks. *Machine Learning*, 20(3):273–297.
- Deif, M. A., Attar, H., Amer, A., Elhaty, I. A., Khosravi, M. R., Solyman, A. A., et al. (2022). Diagnosis of oral squamous cell carcinoma using deep neural networks and binary particle swarm optimization on histopathological images: an aiomt approach. *Computational Intelligence and Neuroscience*, 2022.
- Ferro, A., Kotecha, S., and Fan, K. (2022). Machine learning in point-of-care automated classification of oral potentially malignant and malignant disorders: a systematic review and meta-analysis. *Scientific Reports*, 12(1):13797.
- He, K., Zhang, X., Ren, S., and Sun, J. (2015). Deep residual learning for image recognition.
- Khan, A. M., Rajpoot, N., Treanor, D., and Magee, D. (2014). A nonlinear mapping approach to stain normalization in digital histopathology images using image-specific color deconvolution. *IEEE Transactions on Biomedical Engineering*, 61(6):1729 – 1738. Cited by: 391; All Open Access, Bronze Open Access.
- Kim, Y.-D., Park, E., Yoo, S., Choi, T., Yang, L., and Shin, D. (2016). Compression of deep convolutional neural networks for fast and low power mobile applications.
- Kolda, T. G. and Bader, B. W. (2009). Tensor decompositions and applications. *SIAM Review*, 51(3):455–500.
- Kumar, V., Abbas, A., Fausto, N., and Aster, J. (2009). *Robbins & Cotran Pathologic Basis of Disease E-Book*. Robbins Pathology. Elsevier Health Sciences.
- Liu, Y. and Ng, M. K. (2022). Deep neural network compression by tucker decomposition with nonlinear response. *Knowledge-Based Systems*, 241:108171.
- Lumerman, H., Freedman, P., and Kerpel, S. (1995). Oral epithelial dysplasia and the development of invasive squamous cell carcinoma. *Oral Surgery, Oral Medicine, Oral Pathology, Oral Radiology, and Endodontology*, 79(3):321–329.
- Martinez, E. Z., Neto, F. L., and de Bragança Pereira, B. (2003). A curva roc para testes diagnósticos.
- Mitchell, T. M. (1997). Machine learning.
- Neves, L. A., Martinez, J. M. C., Longo, L. H. d. C., Roberto, G. F., Tosta, T. A. A., Faria, P. R. d., Loyola, A. M., Cardoso, S. V., Silva, A. B., Nascimento, M. Z. d., et al. (2023). Classification of h&e images via cnn models with xai approaches, deepdream representations and multiple classifiers. In *Proceedings*.
- Quinlan, J. R. (1986). Induction of decision trees. *Machine Learning*, 1(1):81–106.
- Ribeiro, M. G., Neves, L. A., Roberto, G. F., Tosta, T. A., Martins, A. S., and Do Nascimento, M. Z. (2018). Analysis of the influence of color normalization in the classification of non-hodgkin lymphoma images. In *2018 31st SIBGRAPI Conference on Graphics, Patterns and Images (SIBGRAPI)*, pages 369–376. IEEE.
- Sarwinda, D., Paradisa, R. H., Bustamam, A., and Anggia, P. (2021). Deep learning in image classification using residual network (resnet) variants for detection of colorectal cancer. *Procedia Computer Science*, 179:423–431. 5th International Conference on Computer Science and Computational Intelligence 2020.
- Sethi, A., Sha, L., Vahadane, A. R., Deaton, R. J., Kumar, N., Macias, V., and Gann, P. H. (2016). Empirical comparison of color normalization methods for epithelial-stromal classification in h and e images. *Journal of Pathology Informatics*, 7(1):17.
- Sha, L., Schonfeld, D., and Sethi, A. (2017). Color normalization of histology slides using graph regularized sparse NMF. In Gurcan, M. N. and Tomaszewski, J. E., editors, *Society of Photo-Optical Instrumentation Engineers (SPIE) Conference Series*, volume 10140 of *Society of Photo-Optical Instrumentation Engineers (SPIE) Conference Series*, page 1014010.
- Sidiropoulos, N. D., De Lathauwer, L., Fu, X., Huang, K., Papalexakis, E. E., and Faloutsos, C. (2017). Tensor decomposition for signal processing and machine learning. *IEEE Transactions on Signal Processing*, 65(13):3551–3582.
- Silva, A. B., De Oliveira, C. I., Pereira, D. C., Tosta, T. A., Martins, A. S., Loyola, A. M., Cardoso, S. V., De Faria, P. R., Neves, L. A., and Do Nascimento, M. Z. (2022). Assessment of the association of deep features with a polynomial algorithm for automated oral epithelial dysplasia grading. In *2022 35th SIBGRAPI Conference on Graphics, Patterns and Images (SIBGRAPI)*, volume 1, pages 264–269. IEEE.
- Talo, M. (2019). Convolutional neural networks for multi-class histopathology image classification. *ArXiv*, abs/1903.10035.
- Tosta, T. A. A., de Faria, P. R., Neves, L. A., and do Nascimento, M. Z. (2019a). Computational normalization of h&e-stained histological images: Progress, challenges and future potential. *Artificial intelligence in medicine*, 95:118–132.
- Tosta, T. A. A., de Faria, P. R., Servato, J. P. S., Neves, L. A., Roberto, G. F., Martins, A. S., and do Nascimento, M. Z. (2019b). Unsupervised method for normalization of hematoxylin-eosin stain in histological images. *Comput Med Imaging Graph*, 77:101646.
- Vahadane, A., Peng, T., Albarqouni, S., Baust, M., Steiger, K., Schlitter, A. M., Sethi, A., Esposito, I., and Navab, N. (2015). Structure-preserved color normalization for histological images. In *2015 IEEE 12th International Symposium on Biomedical Imaging (ISBI)*, pages 1012–1015.
- Wild, C., Stewart, B., Weiderpass, E., for Research on Cancer, I. A., and Weltgesundheitsorganisation (2020). *World Cancer Report: Cancer Research for Cancer Prevention*. International Agency for Research on Cancer.
- Wright, M. N., Ziegler, A., and König, I. R. (2016). Do little interactions get lost in dark random forests? *BMC bioinformatics*, 17(1):145.